—Regular Articles—

# Crystalline Drug Aconitine-loaded Poly(d,l-Lactide-CoGlycolide) Nanoparticles: Preparation and *in Vitro* Release

Xuefan XU, Qingyu XIANG, Zhiyao HE, Yuehua LIU, Dan ZHOU, Xuan QIN, Tingting FAN, Zhirong ZHANG, and Yuan HUANG*

*Key Laboratory of Drug Targeting of the Ministry of Education, West China School of Pharmacy, Sichuan University, No. 17, Block 3, Southern Renmin Road, Chengdu 610041, P. R. China*

(Received June 28, 2009; Accepted November 6, 2009)

This paper reports both the optimization of aconitine entrapment and its release from biodegradable poly(d,l-lactide-coglycolide) (PLGA) nanoparticles prepared using the O/W single-emulsion/solvent-evaporation technique. The influence of several parameters, such as the initial aconitine mass, aqueous-phase pH, volume ratio of aqueous/organic phase (W/O), PLGA concentration in the organic phase, *etc.*, on aconitine encapsulation were investigated. The optimized nanoparticles had an entrapment efficiency of 88.40±3.02% with drug loading capacity of 9.42±2.93%. Crystallization growth, which played a crucial role in hindering the incorporation of aconitine into the polymer carrier, was proposed. Differential scanning calorimetry and X-ray powder diffraction demonstrated that aconitine existed in an amorphous state or as a solid solution in the polymeric matrix. The *in vitro* release profiles exhibited a sustained release of aconitine from nanoparticles and a pH-dependent character in phosphate-buffered saline with different pH values. Moreover, aconitine-loaded PLGA nanoparticles could lead to improvement in the stability of aconitine. This work demonstrated the feasibility of encapsulating aconitine into PLGA nanoparticles using the O/W single-emulsion/solvent-evaporation technique.

**Key words**——aconitine, crystalline drug, nanoparticle, poly(d,l-lactidecoglycolide), stability, sustained release

## INTRODUCTION

Aconitine (Fig. 1), a crystalline drug, is the main alkaloid in plants of the genus Aconitum. Although its clinically therapeutic mechanism remains obscure,[1] the extracts of Aconitum plants are widely used in clinic in China and other East Asian countries[2] owing to the good effect against pain and inflammations.[3,4] Additionally, in *in vitro* tests in the human tumor cell lines of the National Cancer Institute, USA, the IC50 value of aconitine (NSC 56464) in the SNB-75 cell line that originated from a central nervous system tumor, was less than 100 $\mu$M, therefore warranting further investigations on its applications in the treatment of cancer. Aconitine is currently commercially available in various pharmaceutical forms, such as injections, capsules, *etc.* However, poor solubility in water (approximately 20 $\mu$g/ml)[5] and in physiologically acceptable organic solvents and instability problems induced by hydrolysis[6] present serious obstacles in the formulation of aconitine. Aconitine injection, which is extensively applied in treating advanced carcinomatous pain clinically, was reported to have many disadvantages such as serious adverse effects, short storage time due to instability, and patient low compliance caused by the need for high-frequency administration. As a consequence, it would be useful to develop a feasible, effective strategy to address these problems and thus increase the effects of aconitine.

Novel drug-delivery systems such as biodegradable nanoparticles may be an alternative approach to achieve the above aim. Nanoparticle drug-delivery systems can be devised to regulate drug release, modulate biodistribution, and improve bioavailability by increasing solubility and stability.[7] For example, bulleyaconitine A, another diterpenoid alkaloid

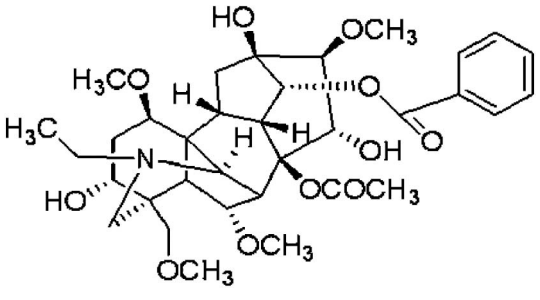


Fig. 1. Chemical Structure of Aconitine

*e-mail: huangyuan0@yahoo.com.cn

of which the chemical structure, physicochemical properties, and pharmacologic actions are similar to those of aconitine, was reported to be incorporated into multivesicular liposomes to obtain sustained-release effects and increase the therapeutic efficiency.[8] Although Dong *et al.*[9] prepared aconitine-loaded liposomes with high drug entrapment efficiency (EE), no related *in vitro* release studies were reported. Aconitine-loaded albumin microspheres were also prepared by our group[10] and exhibited good sustained release *in vitro*, although drug loading (DL) was too low and when drug release was calculated based on the amount of $^{3}$H-labeled aconitine, the *in vitro* release behavior of aconitine was not stimulated sufficiently. In addition, because aconitine is a crystalline drug, it is also difficult to encapsulate into nanoparticles.[11–13] Hence, incorporating a crystalline drug into nanoparticles using an adapted preparation method while achieving delayed release represents a real challenge.

Consequently, the goal of this study was to optimize the encapsulation of aconitine into poly(d,l-lactide-CoGlycolide) (PLGA) nanoparticles to obtain both high drug encapsulation efficiency and sustained drug-release profiles, which would be of great utility for the enhancement of bioavailability and the development of new delivery systems for aconitine. The advantage of employing PLGA as the carrier material lies in its biocompatibility and biodegradability. After stability studies on aconitine under different pH conditions, parameters such as the initial aconitine mass, aqueous-phase pH, volume ratio of the aqueous/organic phase (W/O), PLGA concentration in the organic phase, volume ratio of the acetone/dichloromethane (A/D), and polyvinyl alcohol (PVA) concentration in the aqueous phase were investigated. The mechanism of encapsulation was studied using differential scanning calorimetry (DSC) and X-ray powder diffraction (XRPD) methods. The *in vitro* release of the optimized formulation was evaluated under sink conditions.

## EXPERIMENTAL

**Chemicals and Reagents** Aconitine of 96.1% purity (batch no. 08041202) was purchased from Xi'an Shanchuan Biotechnology Co., Ltd., China. PLGA (lactide/glycolide ratio, 80/20; MW, 15 kDa; batch no. 20071005) was obtained from the Department of Medical Polymers Shandong Institute, China. PVA 205 (88% hydrolyzation degree, 500 polymerization degree) was supplied by Kuraray Co., Ltd., China. All other chemicals and solvents used in this study were of reagent grade.

**pH Stability Studies** PBS (0.1 M, pH 6.0, 7.4, 8.0) was used to study the effects of pH on the stability of aconitine. A stock solution of aconitine was prepared in methanol (100%), and an aliquot (0.2 ml) of this solution was added to 40 ml of each buffer and incubated at 37°C. At various times, samples (in triplicate) of each solution were analyzed for aconitine content using high-performance liquid chromatography (HPLC) with a mobile phase of methanol/water/diethylamine (v/v/v=75/25/0.1) at a flow rate of 0.9 ml/min at 35°C. The analysis used a Diamonsil C18 (5-$\mu$m, 250-mm×4.6-mm) reverse-phase column (Dikma Technologies Beijing, China), an Alltech Model 426 HPLC pump, a Lab. Alliance Model 500-UV absorbance detector at 230 nm, and an Allchrom plus Client/Sever data operator. The injection volume was 20 $\mu$l.

**Nanoparticle Preparation** Nanoparticles were prepared according to the O/W single emulsion/solvent evaporation technique. Typically, PLGA polymer and aconitine are dissolved in an acetone/dichloromethane (v/v) mixture to form the organic phase. The aqueous phase was PVA 205 solution (w/v). Then the organic phase was emulsified with the aqueous phase by sonication using a microtip probe sonicator (JY92-II ultrasonic processor, Ningbo Scientz Biotechnology Co., Ltd., China). The organic solvent was immediately eliminated by rotary vacuum evaporation at 25°C. The initial aconitine mass, aqueous-phase pH, volume ratio of the aqueous/organic phase (W/O), PLGA concentration in the organic phase, volume ratio of acetone/dichloromethane (A/D), and PVA concentration in the aqueous phase were investigated in a single-factor screening experiment. Unless otherwise mentioned, all the experiments are carried out by varying one of the variables while keeping all the other processing variables constant: 4 $\mu$M of aconitine and 30 mg of PLGA (L : G, 80/20; MW, 15 kDa) in 1.5 ml of acetone/dichloromethane mixture (v/v=1) as the organic phase, and 4.5 ml of 1% PVA 205 solution as the aqueous phase. Sonication was carried out at an energy output of 120 W for 2 min in an ice bath. The resultant samples were then purified by filtration through a 0.45-$\mu$m cellulose acetate filter membrane

to remove unincorporated drug crystals as well as copolymer aggregates. Blank nanoparticles were prepared according to the same procedure omitting the drug. All batches of nanoparticles were produced at least in triplicate.

**Determination of DL and EE of Aconitine** To determine DL, the nanoparticle suspension was ultracentrifuged for 1 h at 25℃ (22 000×g, Allegra X-22R Centrifuge, Beckman Coulter Inc., USA) and then the nanoparticle sediments obtained were lyophilized. Appropriate amounts of the lyophilized nanoparticle sediments were accurately weighed and then mixed with 3 ml of acetonitrile. The mixture was vortexed vigorously. After centrifugation at 25℃ (92 ×g) for 10 min, 20 $\mu$l of the obtained supernatant was analyzed using HPLC and the actual amount of aconitine incorporated into PLGA nanoparticles was obtained. DL was calculated based on the percentage of the actual amount of aconitine incorporated into nanoparticles as a ratio of the total amount of lyophilized nanoparticle sediments.

To determine EE, the nanoparticle suspension was divided into two equal parts. One part was mixed with 5 ml of acetonitrile, and the total amount of aconitine in the nanoparticle suspension was determined. The other part was ultracentrifuged for 1 h at 25℃ (22 000×g), and then the obtained supernatant was diluted with acetonitrile and further centrifuged. The amount of aconitine in the supernatants was determined. EE was calculated based on the percentage of the actual amount of aconitine incorporated into nanoparticles as a ratio of the total amount of aconitine in the nanoparticle suspension. Experiments were performed in triplicate.

**Particle Size and Zeta Potential Analysis** The mean particle size (Z-average) of the nanoparticle colloidal suspension was determined using a photon correlation spectroscope (Malvern Zeta-Size Nano ZS90, UK). The suspension was diluted appropriately with double-distilled water before each analysis. The zeta potential was measured using the same instrument following the same dilution in NaCl solution 1 mM. Each measurement was performed in triplicate.

**Optical Microscopy** Nanoparticle colloidal suspensions were placed between glass slides and observed with an Axiovert 40 inverted microscope (Carl Zeiss Shanghai Co., Ltd.) equipped with a Pixera Penguin 150CL-COOLED CCD digital camera systems (Pixera, USA).

**Transmission Electron Microscopy** The morphology of nanoparticles was investigated using transmission microscopy (TEM, H-600IV, Hitachi, Japan). Before analysis, the samples were diluted (1∶5), stained with 2% (w/v) phosphotungstic acid, and placed on copper grids with films for observation.

**DSC and XRPD** After crystal elimination, the nanoparticle colloidal suspension was subjected to ultracentrifugation (22 000×g for 1 h) to remove the free aconitine, and then the nanoparticle sediments obtained were freeze-dried. The lyophilized nanoparticles were accurately weighed in aluminum sample pans and then analyzed on a differential scanning calorimeter (EXSTAR6000 DSC, Japan). The samples were heated at the speed of 10℃/min in the range of 60–250℃ under a nitrogen atmosphere at a flow rate of 50 ml/min. XRPD patterns were obtained using a PHILIPS X'Pert Pro MPD DY1291 diffractometer. The samples were analyzed in the range of 5–50° ($2\theta$). Free aconitine, blank nanoparticles and the physical mixture of the two substances (the proportion was consistent with that in optimized nanoparticles) was chosen as a reference.

***In Vitro* Release of Nanoparticles** After crystal elimination, ths nanoparticle colloidal suspension was diluted to a concentration of 150 $\mu$g/ml with double-distilled water, transferred into the dialysis sac (8～12 KDa, Serua, Germany), and dialyzed against 40 ml of phosphate-buffered saline (PBS) 0.1 M. During the dialysis, a constant temperature culturing shaking incubator (ZHWY-103B, Shanghai Zhicheng Analytical Instrument Manufacturing Co., Ltd.) was used, which was set at 37±1℃ and mechanically shaken at 70 rpm. At designated time internals, 0.5 ml of dialysis medium was collected for measurement and the same volume of fresh medium was added. The amount of released aconitine was determined with HPLC using the method described previously in Section ''pH stability studies''. To evaluate the influence of medium pH on release behavior, PBS 0.1 M with different pH values, *i.e.*, 6.0, 7.4, and 8.0, were investigated. Experiments were performed in triplicate.

**Statistical Analyses** Multivariate data analysis was performed using multiple linear regression on Statistical Product and Service Solutions software (SPSS V11.0, SPSS Inc., USA).

## RESULTS AND DISCUSSION

As a crystalline drug, aconitine was difficult to incorporate into solid lipid nanoparticles in our preliminary experiments. Therefore, in this study, to optimize the encapsulation of aconitine into PLGA nanoparticles using the O/W single-emulsion/solvent-evaporation technique, the effects of six parameters, the initial aconitine mass, aqueous-phase pH, volume ratio of the aqueous/organic phase (W/O), PLGA concentration in the organic phase, volume ratio of acetone/dichloromethane (A/D), and PVA concentration in the aqueous phase, on aconitine encapsulation were systematically investigated.

**Effect of Preparation Parameters on Formulation Characteristics** The effects of six formulation variables on particle size and EE of nanoparticles are shown in Figs. 2–4. Data of the effects of PLGA concentration in the organic phase, the volume ratio of acetone/dichloromethane (A/D) and the PVA concentration in the aqueous phase, which had no significant effects on the aconitine EE, are not shown. The particle size of the nanoparticles had a positive relationship with the PLGA concentration and W/O volume ratio, and a negative relationship with the A/D volume ratio and PVA concentration. The results of multiple linear regression analysis showed that the PLGA concentration, PVA concentration, A/D volume ratio, and W/O volume ratio were the dominant elements ($p<0.05$, respectively) controlling the particle size, and that the initial aconitine amount and pH value of aqueous phase had no significant effects on particle size. As shown in Figs. 2–4, the EE of aconitine increased with the increase in PLGA concentration and the pH value of the aqueous phase, but decreased with the increase in the PVA concentration, A/D volume ratio, and W/O volume ratio. The results of statistical analysis demonstrated that the initial aconitine amount, pH value of the aqueous phase, and W/O volume ratio were the main variables ($p<0.05$, respectively) governing drug EE.

**Influence of Initial Aconitine Amount** Figure 2 shows that the EE of aconitine first increased dramatically with the increase in the initial aconitine amount, until it reached about 80.85% for an initial aconitine amount of 40 $\mu$M. However, with the further increase in the initial aconitine mass, the EE decreased significantly ($p<0.05$). Considering that aconitine is a crystalline drug, the change in the EE of aconitine with the increase in the initial aconitine was possibly decided by two competing factors: molecular dispersion of the drug within the polymeric matrix; and crystallization growth.[14] The EE first increased because the former dominated over the latter. As the initial aconitine amount increased, the amount of drugs in the organic phase increased and then more drug

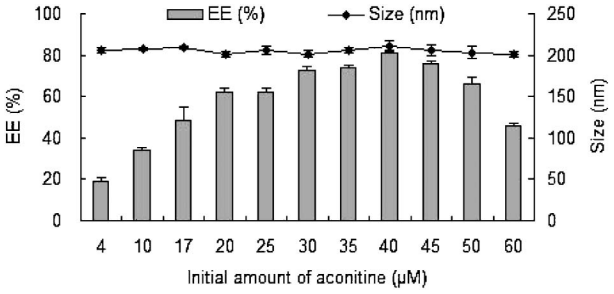


Fig. 2. Effects of the Initial Aconitine Amount on Particle Size (nm) and Entrapment Efficiency (EE, %) of Nanoparticles
Mean±S.D., $n=3$.

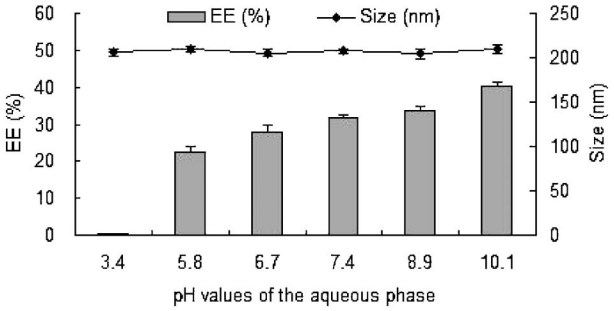


Fig. 3. Effects of the Aqueous-phase pH on Particle Size (nm) and EE (%) of Nanoparticles
Mean±S.D., $n=3$.

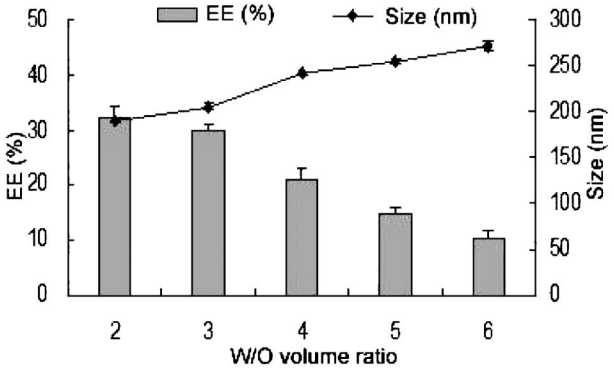


Fig. 4. Effects of Aqueous/Organic Phase (W/O) Volume Ratio on the Particle Size (nm) and EE (%) of Nanoparticles
Mean±S.D., $n=3$.

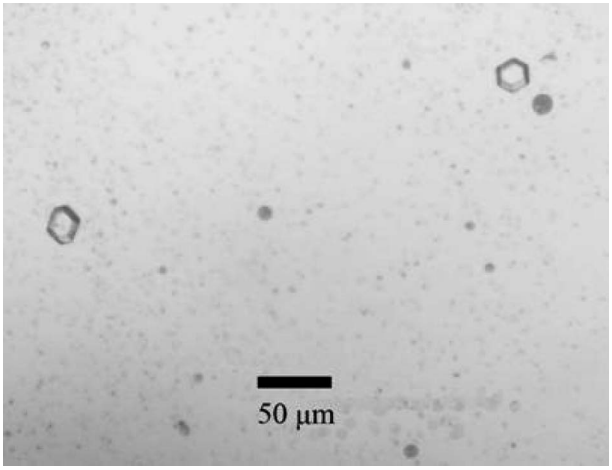


Fig. 5. Optical Microscopy Image of Aconitine Crystals Present in Nanoparticle Suspension

Nanoparticles were prepared with aconitine 17 $\mu$M under constant conditions (original magnification, 10×40; scale bar, 50 $\mu$m).

molecules interacted with the polymeric matrix, resulting in the increase in the amount of aconitine entrapped. Nevertheless, with the increase in aconitine crystals, which was observed in optical microscopy (Fig. 5), crystallization forces progressively dominated over the molecular dispersion of the drug within the polymeric matrix, and thus the EE was reduced, which was confirmed by the finding that as the aconitine amount increased (it was varied between 4 $\mu$M and 60 $\mu$M, which was well below the saturation limit in the organic phase during the experiment), more drug crystals were deposited from the colloidal suspension during the emulsification and solvent-evaporation process. When acetone and dichloromethane were eliminated by evaporation, drug solubility in the dispersion medium decreased, leading to the formation of crystals.[13] As shown in Fig. 2, the particle size was independent of the initial aconitine amount.

**Influence of Aqueous-phase pH** Aconitine is a diterpenoid alkaloid and contains a tertiary amine group (Fig. 1) imparting weak alkalinity to the drug molecule. It is thus easily ionized in acid medium and consequently the aqueous solubility of aconitine is greatly enhanced. Conversely, under basic conditions, the neutral form is the main form of aconitine, and accordingly, its lipid solubility increases significantly. It was therefore reasonable to hypothesize that increasing the aqueous-phase pH and thereby increasing the solubility of aconitine in the internal phase could enhance drug entrapment into nanoparticles. To confirm the hypothesis, studies were subsequently carried out using the aqueous phase with different pH values.

The results are presented in Fig. 3. Obviously, pH affects the EE of aconitine in the polymeric matrix dramatically ($p<0.05$). The change in pH in the aqueous phase had inconsequential effects on particle size. The profiles showed an increasing drug entrapment trend with an increase in the aqueous-phase pH from 3.4 to 10.1. Selecting water pH 3.4 as the internal phase led to only a 0.43% EE, while pH 5.8 significantly increased EE to 22.36%. This occurred because with the increase in the aqueous-phase pH value, the degree of ionization of aconitine was probably reduced[15] and thus the neutral form became the main form of aconitine, especially at pH values greater than the pKa (5.78) of aconitine,[16] which contributes to migration of the drug into the organic phase, hence causing more aconitine retention in the polymeric matrix and resulting in the increase in EE. Although the EE of aconitine reaches the maximum at pH 10.1, the decomposition of PLGA and aconitine[6] could be promoted under such basic conditions, which is unfavorable for storage and administration. Therefore the aqueous-phase pH of 7.4 was employed in the optimized preparation.[17]

**Effects of Aqueous/Organic-phase (W/O) Volume Ratio** The effects of the W/O volume ratio on the particle size and the EE of aconitine are presented in Fig. 4. An increase in the W/O volume ratio resulted in a conspicuous increase in particle size ($p<0.05$) and a notable decrease in drug entrapment ($p<0.05$). The reason for the increase in particle size may be as follows: on the one hand, the coalescence of droplets may be promoted by the gradual reduction in the amount of organic solvent available for diffusion in the O/W emulsion.[18] On the other hand, the increase in the total volume of the aqueous and organic phases would reduce the net shear stress at a constant external energy input, leading to the increase in particle size. Although the W/O volume ratio increased and the total amount of PVA increased correspondingly, resulting in a reduction in interfacial tension and thereby decreasing the nanoparticle size, it was obvious that it was not the dominant factor when the W/O volume ratio was varied between 2 and 6. An increase in the W/O volume ratio may lead to a large quantity of drug molecules partitioning out into the aqueous phase during the emulsification procedure

and fewer drug molecules remaining in emulsion droplets to interact with the polymer molecules, thus decreasing the EE of aconitine.

**Optimization of Nanoparticle Formulation** In addition to exploring the three variables above, the PLGA concentration in the organic phase, acetone/dichloromethane (A/D) volume ratio, and PVA concentration in the aqueous phase were also investigated systematically. The results showed that these parameters had no substantial effect on the aconitine EE (data not shown). Finally, regarding the relatively high EE and DL and small particle size, the optimized aconitine-loaded nanoparticle formulation corresponds to an initial aconitine amount of 40 $\mu$M, 30 mg of PLGA (80 : 20), 1.5 ml of the acetone/dichloromethane mixture (v/v=1), and 3 ml of 1% PVA 205 aqueous solution (w/v) (pH 7.4) as the internal phase and external phase, respectively. The reason for selecting PLGA with the L : G ratio of 80 : 20 as the carrier material lies in the increased hydrophobicity of polymer at higher L : G ratios, which increases the hydrophobic interaction of aconitine with PLGA.[19]

**Characterization of Optimal Nanoparticle Formulation** The zeta potential and size of unloaded nanoparticles and aconitine-loaded nanoparticles did not differ significantly. Both the optimized nanoparticles and unloaded nanoparticles demonstrated similar particle sizes (201±9 nm and 209±6 nm, $n$=3, respectively) and negative zeta potentials (−3.99±0.77 mV and −4.79±0.68 mV, $n$=3, respectively).

The apparent final yield (%), which could be calculated as a percentage of the total amount of lyophilized nanoparticle sediments in the total amount of initial materials, was 79.83±3.46% ($n$=3). The improved on EE of aconitine was confirmed by a relatively high DL rate (9.42±2.93%, $n$=3) and EE (88.40±3.02%, $n$=3). Corresponding TEM studies showed discrete nanoparticles with a spherical shape and smooth surface (Fig. 6).

**DSC and XRPD** To investigate the physical state of aconitine in nanoparticles, DSC analysis was performed on aconitine, blank nanoparticles, aconitine-loaded nanoparticles, and the physical mixture of aconitine and blank nanoparticles. A drug may exist in either an amorphous state or a crystalline state in the polymeric matrix. Furthermore, a drug also may be present either as a solid solution or solid dispersion in an amorphous or crystalline polymer.[20]

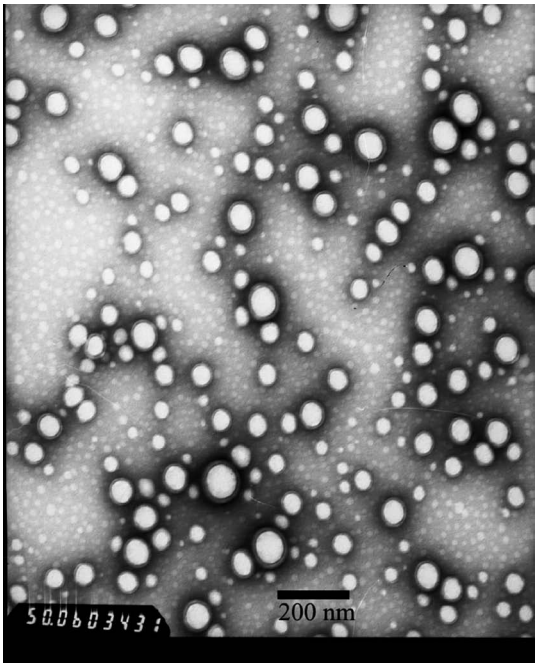


Fig. 6. Transmission Electron Microscopy Photomicrograph of Nanoparticles
Scale bar, 200 nm.

DSC curves are presented in Fig. 7. Comparing the curves of aconitine, blank nanoparticles, aconitine-loaded nanoparticles (with aconitine contents of 5.53% and 9.42%), and the physical mixture (with aconitine contents of 5.53% and 9.42%), it is obvious that pure aconitine showed a single sharp endothermic melting peak at 198.6°C (Fig. 7(F)), which was broadened and slightly shifted to a lower temperature (196.1°C) for the 5.53% and 9.42% aconitine/blank nanoparticle physical mixture (Fig. 7(B), (C)). However, the aconitine melting peak totally disappeared in the curves of the 5.53% and 9.42% aconitine-loaded nanoparticles (Fig. 7(D), (E)), indicating the absence of crystalline drug in the aconitine-loaded samples, at least at the particle surface level. The polymer may have inhibited the crystallization of aconitine during nanoparticle formation. Hence, it could be concluded that aconitine formulated in the nanoparticles was in an amorphous or disorderly crystalline phase of a molecular dispersion or a solid solution state in the polymer carriers.[21]

In addition, XRPD analysis was used to determine the crystalline content of aconitine in the nanoparticles. The graphs depicted in Fig. 8 show the XRPD patterns of aconitine, blank nanoparticles, aconitine-loaded nanoparticles, and the physical mixture of aconitine and blank nanoparticles. It appeared that

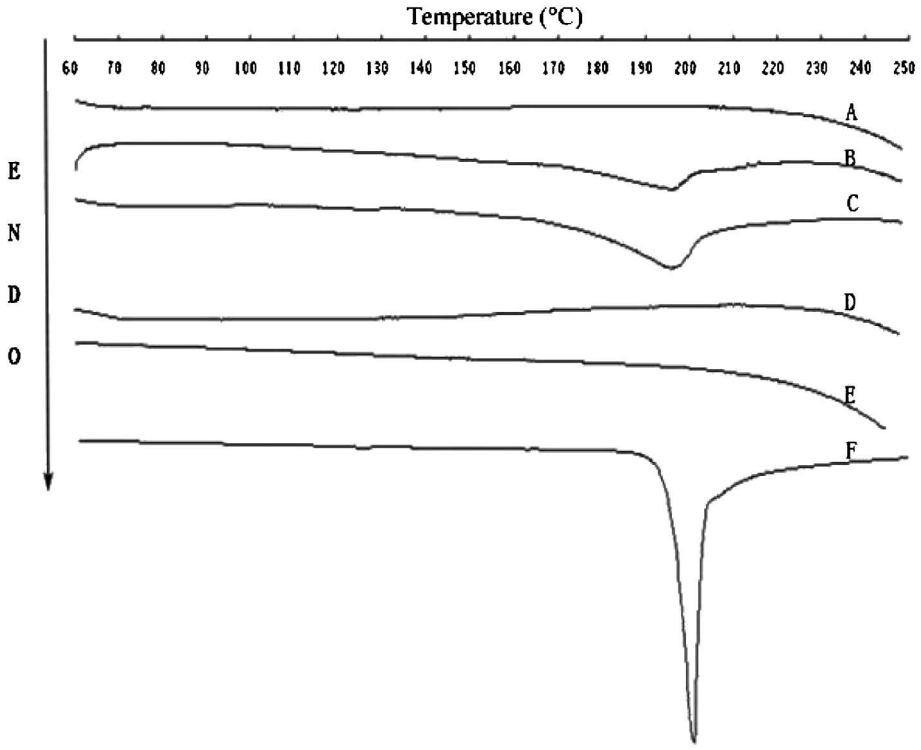


Fig. 7. DSC Analysis

DSC thermograms of blank nanoparticles (A), the physical mixture of aconitine and blank nanoparticles (B, 5.53%, w/w), the physical mixture of aconitine and blank nanoparticles (C, 9.42%, w/w), aconitine-loaded nanoparticles (D, 9.42%, w/w), aconitine-loaded nanoparticles (E, 5.53%, w/w), and aconitine (F).

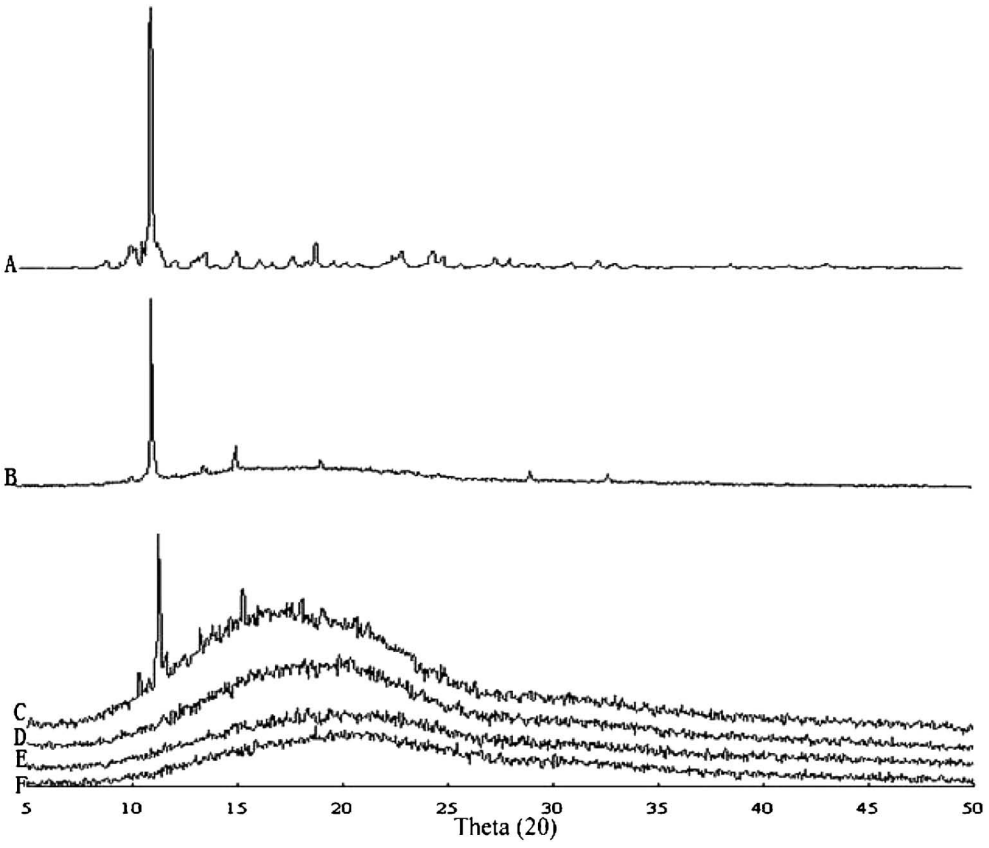


Fig. 8. XRPD Analysis

XRPD diffraction patterns of aconitine (A), the physical mixture of aconitine and blank nanoparticles (B, 9.42%, w/w), the physical mixture of aconitine and blank nanoparticles (C, 5.53%, w/w), blank nanoparticles (D), aconitine-loaded nanoparticles (E, 9.42%, w/w), and aconitine-loaded nanoparticles (F, 5.53%, w/w).

blank nanoparticles (Fig. 8(D)) were in an amorphous state and that aconitine powder (Fig. 8(A)) was crystalline. The crystal diffraction peaks of aconitine were still visible for the 5.53% and 9.42% aconitine/blank nanoparticle physical mixture (Fig. 8(B), (C)). Nevertheless, no crystalline diffraction pattern was distinguishable in the graphs of the 5.53% and 9.42% aconitine-loaded nanoparticles (Fig. 8(E), (F)), indicating that aconitine was present in the nanoparticles in an amorphous state, which was consistent with the results of DSC analysis.

**pH Stability Studies and *in Vitro* Aconitine Release from Nanoparticles** Aconitine contains ester moieties in the molecule (Fig. 1) and is easily hydrolyzed to form more polar compounds.[6,22] Considering pH as one of the main factors affecting aconitine hydrolysis, which would affect its release from nanoparticles, the pH stability of aconitine in PBS was investigated. The results were shown in Fig. 9. At pH 6.0, about 52.98% of the aconitine still remained in hydrolysis medium during 56-h incubation. However, there was nearly 100% decomposition of aconitine in the weakly alkaline PBS solutions (pH 7.4, 8.0) after incubating for 22 h and 8 h, respectively. Obviously, compared with weakly acidic conditions, aconitine was more unstable under weakly basic conditions and the increasing basicity in the medium solution markedly promoted the degradation of aconitine at 37℃.

The profiles of aconitine release from nanoparticles at different pH values are presented in Fig. 10(A) and (B). Figure 10(A) shows that at pH 6.0 a 32.02% release occurred within the first 6 h of incubation, followed by a relatively slow-release phase, and 78.69% of the active drug was released after 56 h of incubation. Despite the two crystalline drugs (aconitine and dexamethasone) exhibiting similar poor solubility in water, the release of aconitine shown here was much slower than that of the dexamethasone-loaded PLGA nanoparticles prepared using a similar emulsification/evaporation method,[14] in which about 100% of dexamethasone was released in 4 h under sink conditions. At pH 6.0, the 32.02% release at the initial stage proceeded by means of both the hydration of the interfacial aconitine molecules and their passive diffusion; the relatively slow-release phase after the first few hours of incubation may be attributed to the drug incorporated into the inner core of nanoparticles.

As presented in Fig. 10(B), the drug release from

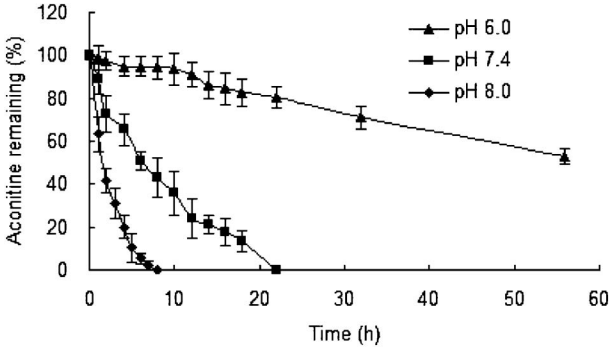


Fig. 9. pH Profile Stability of Aconitine in PBS at 37℃
pH 6.0 (▲); pH 7.4 (■); pH 8.0 (◆). Mean±S.D., $n=3$.

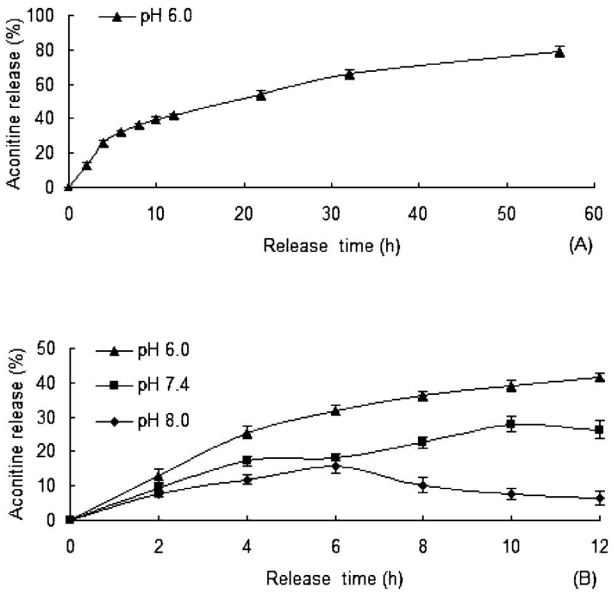


Fig. 10. *In Vitro* Release Profile of Aconitine from Nanoparticles in PBS at Different pH Values
(a) pH 6.0; (b) three different pH values (6.0, 7.4, 8.0). Mean±S.D., $n=3$.

nanoparticles reached the maximum after 10 h (pH 7.4) and 6 h (pH 8.0) of incubation in the release medium and then decreased gradually. This occurred possibly because the decomposition rate of aconitine in weakly alkaline solutions dominated over the drug release velocity by degrees with the passage of incubation time. However, aconitine is so stable in acidic aqueous solution that the drug release amount at pH 6.0 increased continuously in a time span of 12 h. Compared with Fig. 9, Fig. 10(A) shows that at pH 6.0, the drug release amount (78.69%) was much greater than that of the residual drug (52.98%) in the same incubation time period (56 h). Similarly, at pH 7.4, compared with 26.35% of aconitine released from nanoparticles, only 23.90% remained after

hydrolysis in the first 12 h of incubation time; aconitine totally decomposed in the hydrolytic solution at pH 8.0 while 10.23% of drug remained in the release medium (8 h). These results indicated that the incorporation of aconitine into PLGA nanoparticles could lead to improvement in the stability of aconitine.

In addition, the pH dependence of drug release illustrated in Fig. 10(B) is a remarkable phenomenon. The rate of drug release had a negative relationship with the release medium pH. This can be explained by the difference in the solubility characteristics of aconitine under acidic and alkaline conditions. Because of the ionization of drug molecules in acidic pH medium, the solubility of aconitine greatly increased, which promoted the diffusion of aconitine from the particle surface to the release medium. On the contrary, the neutral form is the main form of aconitine in alkaline pH medium, thereby resulting in the poor solubility of aconitine, which hinders faster release.

In conclusion, aconitine-loaded PLGA nanoparticles with fairly high EE and DL were prepared for the first time using an O/W single-emulsion/solvent-evaporation technique. We assessed the effects of six formulation parameters on drug entrapment. From the analyses of the different changing trends with the change in formulation variables presented by the EE, both the chemical interaction between the polymer molecules and drug molecules and the migration of drug into the external aqueous phase are crucial factors controling the drug incorporation efficiency. Crystallization growth, which plays a vital role in hindering the incorporation of aconitine into the polymer matrix, is proposed. Additionally, the *in vitro* drug release profiles indicated that the sustained release of aconitine from nanoparticles was achieved and aconitine-loaded PLGA nanoparticles could lead to improvement in the stability of aconitine in PBS at different pH values. The results of this study demonstrate the feasibility of encapsulating aconitine into PLGA nanoparticles using the O/W single-emulsion/solvent-evaporation technique, which indicates that the potential carrier of the nanoparticle delivery system for aconitine is feasible and could provide valuable references for subsequent research on aconitine and a series of diterpenoid alkaloids similar to aconitine in structure and physicochemical properties.

**Acknowledgments** This research was supported by financial assistance from the Ministry of Education (NCET-06-0786) and National High-tech R&D Program (863 Program, 2007AA021801) of PR China.

## REFERENCES

1) Hikino H., Ito T., Yamada C., Sato H., Konno C., Ohizumi Y., *J. Pharmacobiodyn.*, **2**, 78–83 (1979).
2) Zhang H. G., Sun Y., Duan M. Y., Chen Y. J., Zhong D. F., Zhang H. Q., *Toxicon*, **46**, 500–506 (2005).
3) Bisset N. G., *J. Ethnopharmacol.*, **4**, 247–336 (1981).
4) Han G. Q., Chen Y. Y., Liang X. T., "The Alkaloids, Distribution of alkaloids in traditional Chinese medicine plants," ed. by Brossi A. Academic Press, New York, 1988, pp. 241–227.
5) Jones G. L., Wimbish G. H., McIntosh W. E., *Med. Res. Rev.*, **3**, 383–434 (1983).
6) Huang J., Wang X. H., Wu T. T., *Acta Pharm. Sin.*, **20**, 933–939 (1985).
7) Goldberg M., Langer R., Jia X. Q., *J. Biomater. Sci. Polymer Ed.*, **3**, 241–268 (2007).
8) Lu W. G., Chen T. T., Ren D. Q., *Chin. Trad. Pat. Med.*, **26**, 825–827 (2007).
9) Dong W. W., Zhang Y. F., Liu X. P., Geng D. Q., *J. Chin. Med. Mat.*, **31**, 31–33 (2008).
10) Huang Y., Hou S. X., Lin J. N., *China J. Chin. Mat. Med.*, **22**, 731–733 (1999).
11) Brigger I., Chaminade P., Marsaud V., Appel M., Besnard M., Gurny R., Renoir M., Couvreu P., *Int. J. Pharm.*, **214**, 37–42 (2001).
12) Dong Y., Feng S. S., *Biomaterials*, **25**, 2843–2849 (2004).
13) Layre A. M., Gref R., Richard J., Requier D., Chacun H., Appel M., Domb A. J., Couvreur P., *Int. J. Pharm.*, **298**, 323–327 (2005).
14) Gómez-Gaete C., Tsapis N., Besnard M., Bochot A., Fattal E., *Int. J. Pharm.*, **331**, 153–159 (2007).
15) Govender T., Stolnik S., Garnett C. M., Illum L., Davis S. S., *J. Control. Release*, **57**, 171–185 (1999).
16) Webb M. R., Ebeler S. E., *Biochem. J.*, **384**, 527–541 (2004).
17) Bodmeier R., McGinity J. W., *J. Microencap-*

*sul.*, **4**, 289–297 (1987).
18) Mainardes R. M., Evangelista R. C., *Int. J. Pharm.*, **290**, 137–144 (2005).
19) Budhian A., Siegel S. J.,Winey K. I., *Int. J. Pharm.*, **336**, 367–375 (2007).
20) Musumeci T., Ventura C. A., Giannone I., Ruozi B., Montenegro L., Pignatello R., Puglisi G., *Int. J. Pharm.*, **325**, 172–179 (2006).
21) Dubernet C., *Thermochim. Acta*, **248**, 259–269 (1995).
22) Mizugaki M., Ito K., Ohyama Y., Konishi S., Tanaka S., Kurasawa K., *J. Anal. Toxicol.*, **22**, 336–340 (1998).